Available online at www.sciencedirect.com

ScienceDirect

Ciência & Tecnologia dos MATERIAIS

http://ees.elsevier.com/ctmat

Ciência & Tecnologia dos Materiais 29 (2017) e108–e113

Special Issue "Materiais 2015"

Design of a self-contained breathing apparatus (SCBA) using a carbon fibre reinforced polymer and filament winding

L. Fernandes[a,*], Rui F. Martins[b], Paulo P. Silva[a]

[a]*Escola Naval, CINAV, Base Naval de Lisboa, Alfeite, 2810-001 Almada, Portugal*

[b]*UNIDEMI, Faculty of Sciences and Technology, Universidade Nova de Lisboa, Campus de Caparica, 2829-516 Caparica, Portugal*

Abstract

The design of a self-contained breathing apparatus (SCBA), which is an extremely important device for firefighting on board of ships, covers not only in-service loadings, but also a proper selection of materials, manufacturing processes, as well as the specification of other construction details, such as hydrostatic test parameters, among others.

The work developed and presented in this manuscript sought to verify the feasibility and the advantages of using composite materials in a SCBA subjected to high internal pressure (300 bar, 30 MPa), instead of other metallic material currently in use. Hence, a carbon fibre reinforced polymer (CFRP) and the filament winding technique were considered in the SCBA redesign. Analytical formulas, as well as engineering standards and advanced finite element analysis (FEM) were used to analyse two types of SCBA commonly used on board of ships.

Five valid axial tensile tests were performed in samples of CFRP using a DARTEC 100 kN servo hydraulic machine according with standard ASTM D3039/D 3039M (2002) in order to determine the mechanical properties of the material, and a displacement transducer or strain gages were used to determine strains induced in the composite during experimental axial tensile tests, Then, several FE numerical simulations were carried out in order to verify the compliance of a redesigned SCBA with the functional requirements, and the main manufacturing parameters were also determined. Furthermore, experimental internal pressure tests were carried out in a pressure vessel similar to the redesigned SCBA. The results of FE simulations and experimental tests were compared and conclusions could be drawn.

Keywords: Carbon fibre reinforced polymer (CFRP); filament winding; self-contained breathing apparatus (SCBA); strain-gauges; finite element analysis (FEA).

1. Introduction

Materials are the basis of all natural and man-made structures. Therefore, nowadays, technology and science development, associated with continuous improvement of existing material properties, as well as with the expansion of structural materials classes and types, causes new combinations of materials to emerge. Usually, new materials are developed due to the need to improve structural efficiency and performance, being, simultaneously, as economically profitable as possible. One of the best manifestations of this process of development of materials, structures and technology is associated with the increasing use of composite materials that will be the focus of this study.

In fact, the work developed and herein presented sought to verify the feasibility and the benefits that pressure vessel designers can obtain from using CFRP filament winding technique in a specific type of pressure vessel design application.

In order to achieve that purpose, advanced numerical simulations of pressure vessels manufactured either on metallic or on composites materials were carried out using SolidWorks/Simulation and/or ANSYS

* Corresponding author.

E-mail address: freire.fernandes@marinha.pt (L. Fernandes)

http://dx.doi.org/10.1016/j.ctmat.2017.05.001

software, combined with calculation based on analytical formulations and on engineering formulas defined in appropriate standards. To validate the numerical simulations and to get a more in-depth understanding of composite materials mechanical behaviour, strain gauges were applied on a pressure vessel submitted to internal pressure and uniaxial tensile tests of specimens made of composite materials were carried out. Strain-gauges were applied both to pressure vessel and to the specimens.

On the other hand, the design of pressure vessels comprehends not only its dimensioning, in order to resist burst pressure, but also the appropriate materials and manufacturing processes selection, as well as the specification of remaining construction details. Some of this information will also be addressed in this paper.

2. Materials and Methods

2.1. Pressure vessels under study

This research aimed to analyse two specific types of pressure vessels. One of the geometries is a SCBA, which is a pressure vessel manufactured in metallic materials that is used on board of ships in case of fire accident, or other emergency situation that would require the usage of a self-breathing apparatus. This pressure vessel typically comprehends a main cylindrical body - a cylindrical shell was considered [1], with two different types of domes, namely a semi-elliptical dome and a hemispherical dome (Fig. 1).

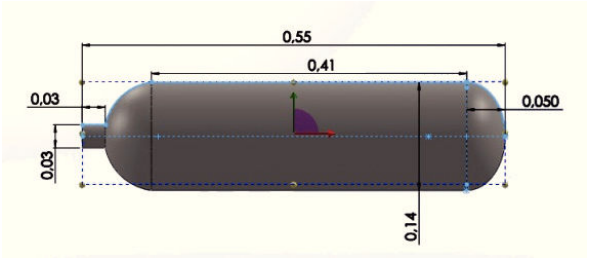

Fig. 1. SCBA's main dimensions (in meters); D_i=0.14 m.

In order to calculate the design thicknesses necessary to withstand internal pressure required (300 bar, 30 MPa), design formulas present in standard ASME Boiler and Pressure Vessel Code – Sec.VIII, Div.1 [2], as well as theory of plates, and shells and the Finite Element Method (FEM), were used. The results obtained by the three different methodologies referred were in good agreement, with an error lower than 5%, and detailed information can be found in [3]. The 10 mm, 20 mm and 13 mm design thicknesses were calculated for the hemispherical dome, the cylindrical surface and the semi-elliptical dome under study, respectively, and the estimated weight of the metallic SCBA was approximately equal to 27 kg.

A second type of pressure vessel, made in composite materials, currently used in sports like paint-ball and airsoft, was modelled (Fig. 2), becoming a reference's geometry for analytical and practical studies that aimed to redesign the metallic SCBA apparatus (Fig. 1). This pressure vessel's geometry was composed by a main cylindrical body, just like the SCBA geometry, and two different domes, namely a hemispherical dome and a torispherical dome. It also has an internal thermoplastic liner, which is used both to support the filament winding during its production and to avoid leak of fluid during functioning. However, the thermoplastic liner has much lower mechanical properties than the composite material and it was not considered. An overall view of a thermoplastic liner specimen after axial test was placed in Fig. 2.

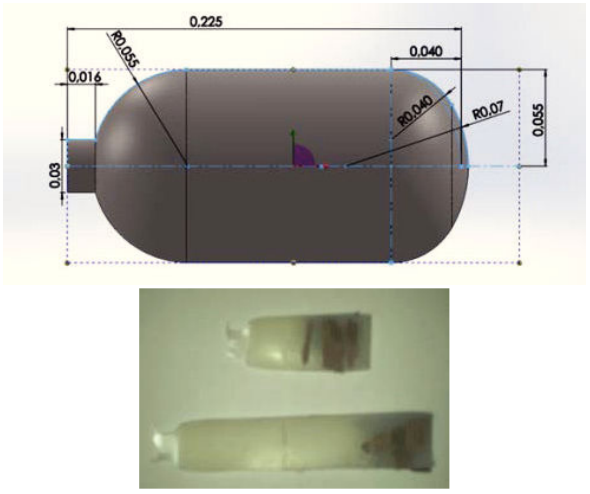

Fig. 2. Dimensions, in meters, of a pressure vessel manufactured in a composite material with an internal thermoplastic liner (overall view of the experimental thermoplastic specimen after axial test).

Both pressure vessels under study were modelled using CAD software.

2.2. Design of pressure vessels in composite material

The design of this kind of pressure vessels involves the application of thin shell's theory along with different methodologies that takes into account the specific usage of composites materials [4,5]. The methodology depends on each author and was extensively analysed on the thesis [3] that supports the study hereby presented.

Considering the following mechanical properties for the composite material [3,4], and taking into account the "SCBA" geometry, the ply thickness [4], T_{PLY}, could be calculated (Eq. 1):

- Reinforcement: PAN Carbon (density ρ_r = 1.7 g/cm^3, Young's modulus E = 294 GPa, Maximum allowable stress 5123 MPa).
- Matrix: Epoxy (density ρ_m = 1.2 g/cm^3, Young's modulus E = 4500 MPa).

$$T_{PLY} = \frac{T_{REF} \text{ x } CSA}{CSA_{REF}} = 0.254 \text{ mm} \quad (1)$$

where CSA = 0.4393 mm^2, T_{REF} = 0.142 mm for a CSA_{REF} = 0.246 mm^2, which are related to tow cross section area, reference thickness, and to reference CSA, respectively [4]. This approach is a useful rule that has its basis in demonstrated experience, as stated in [4].

As the Young's modulus of the reinforcement (fibre) is known, as well as its critical tensile strength (5123 MPa) [4], the maximum hoop strain allowable, ε_{HOOP}, was calculated (Eq. 2):

$$\varepsilon_{HOOP} = \frac{\sigma_{HOOP}}{E_{FIBER}} = 0.0174 \quad (2)$$

In addition, using an appropriate safety factor, FS, of 1.25, and considering an internal pressure of 300 bar (30 MPa), as well as a cylinder inside radius, Rc, of 0.07 m, the axial load expected is given by (Eq. 3) [4]:

$$N_\varphi = FS \text{ x } P \text{ x } Rc \text{ x } \frac{(1+\varepsilon_{HOOP})}{2} = 1334.8 \text{ N/mm} \quad (3)$$

In the same line of thought and considering the factor $(1+\varepsilon_{HOOP})$ as a correction of the inner radius [4], Rc, the hoop load, N_θ, could be obtained (Eq. 4):

$$N_\theta = FS \text{ x } P \text{ x } Rc \text{ x } (1+\varepsilon_{HOOP}) = 2669.6 \text{ N/mm} \quad (4)$$

The fibre volume fraction (Eq. 5) is also an important parameter that determines the strength resistance of composites parts, and, due to practical and operational reasons, it can reach up a maximum value of about 70% [4]. In order to size a carbon/epoxy laminate, design tables that optimize its composition (Fig. 3) are given in [5], and its usage imply the adoption of specific parameters, namely a ply thickness of 0.13 mm and a fibre volume fraction equal to 60% [5].

$$V_F = \frac{1}{1+\frac{W_R}{1-W_R} \text{ x } \frac{\rho_f}{\rho_r}} = 0.596 \approx 60\% \quad (5)$$

where W_R is the resin weight fraction.

Combining the main stresses, N_φ and N_θ (Eqs. 3 and 4) as shown in Fig. 3, the reduced stress resultants were calculated, namely $\overline{N_\varphi}$, $\overline{N_\theta}$, $\overline{T_{xy}}$, and the optimal theoretical composition for the carbon/epoxy laminate suggested in [5] is shown in Fig. 3:

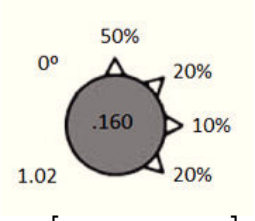

$$\overline{N_\varphi} = N_\varphi / \left[|N_\varphi| + |N_\theta| + |T_{xy}| \right] = 0.(3)$$

$$\overline{N_\theta} = N_\theta / \left[|N_\varphi| + |N_\theta| + |T_{xy}| \right] = 0.(6)$$

$$\overline{T_{xy}} = T_{xy} / \left[|N_\varphi| + |N_\theta| + |T_{xy}| \right] = 0$$

Fig. 3. Optimal composition for the laminate based on resultant stress [5].

The optimal composition of the laminate can be interpreted as follows:

- 50% of +90º plies
- 20% of +45º plies
- 10% of 0º plies
- 20% of -45º plies

- Minimum thickness of the laminate for each 100 N/mm (resulting from the sum of the stress resultants): 0.160 mm.
- For this laminate, the first ply failure will occur in the 0º plies.
- One can continue to load this laminate until it reaches 1.02 times the critical load, as:

$$N_{\varphi r} = 1.02 \text{x} 1334.8$$
$$N_{\theta r} = 1.02 \text{x} 2669.6$$
$$T_{xyr} = 0 \text{ N/mm}$$

which will result in the arithmetic sum ($N_{\varphi r}$+$N_{\theta r}$+T_{xyr}) of 4084.4 N/mm, and in an expectable thickness, (t) according to what was previously described equal to (0.16x4084.4)/100 = 6.54 mm.

- However, the composition of the laminate was calculated under the assumption that the filament-wound laminate is a stacking sequence, but in reality it is a layup of +/- angle plies wit interweaved tows.

- 0º plies are not adequate for filament winding.
- The optimum angles for winding a composite pressure vessel are normally limited by the effective geometry, namely the ratio between the "neck" diameter and the overall diameter and length, and the 45º plies are hardly optimized considering combination of hoop and longitudinal stresses.

In addition, making use of the critical stress (308 MPa) obtained in the experimental tests carried out in five composite specimens (these tests will be explained later in this paper) and considering a wind angle, α_0, of approximately 14.5º (Fig. 1) when assuming helical winding (geodesic) [4], the expected thickness [4] will be about 14 mm, as follows:

$$\alpha_0 \cong \sin^{-1}\left(\frac{0.015+0.0025}{0.07}\right) \cong 14.5^{\circ}$$

$$t_{HOOP} = \frac{N_\theta - N_\varphi \tan^2(\alpha)}{\sigma_{ADM}} \cong 14\ \text{mm}$$

Therefore, the band width (BW) and the number of tows, N_{TOWS}, could be calculated [4] (Eq. 6), considering the bandwidth small compared to the radius of curvature of the pressure vessel:

$$D \times 0.02 \le BW \le D \times 0.04$$

$$2.8\ \text{mm} \le BW \le 0.04$$

$$N_{TOWS} = \frac{BW \times T_{PLY}}{CSA} \begin{cases} \frac{2.8 \times 0.254}{0.4393} = 1.62 \\ \frac{5.6 \times 0.254}{0.4393} = 3.24 \end{cases} \quad (6)$$

$$TPI = \frac{T_{PLY}}{CSA} \therefore\ TPI = 0.578\ \text{tow/mm}$$

Hence, 3 tows per zone, and 0.578 tow/mm, one can obtain the final band width:

$$BW = \frac{N_{TOWS}}{TPI} = 5.19\ \text{mm} \quad (7)$$

3. Experimental Tests and Numerical Simulations

3.1. Experimental tensile tests

In order to determine approximate mechanical properties of similar composite material foreseen to be used in the SCBA manufacture, some tensile tests were performed in CFRP samples using a servo hydraulic machine - model DARTEC 100 kN, according with standard ASTM D3039/D 3039M (2002) [6]. The rectangular samples, of 25x15 mm, were tested with a load rate of 0.1 and 0.2 kN/s.

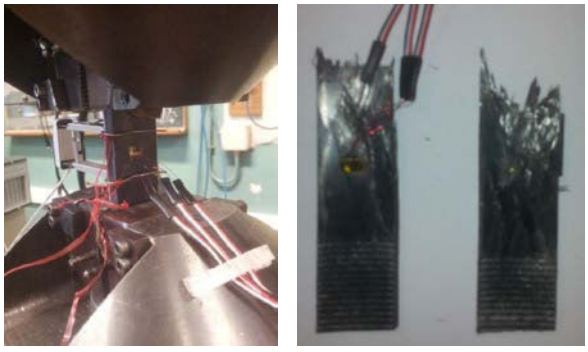

Fig. 4. Experimental tensile tests.

In all tests carried out a transducer of displacement (ΔL) was used, and in some tests it was also used a strain gage rosette (120.0 Ω ± 0.6%) to validate experimental strain results (Fig. 4). This gage had three grids, with the second and third grids angularly displaced from the first grid by 45º and 90º, respectively (Fig. 5). The equations for calculating principal strains from the rosette strain measurements are derived from what is known as the "strain-transformation" relationship [7].

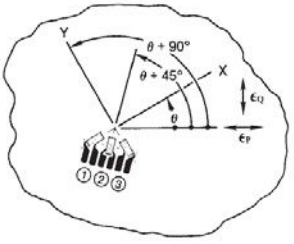

Fig. 5. Rectangular rosette, with grid n.1 at the arbitrary angle θ from the major principal axis.

Hence, strains sensed by each grid, namely ε_1, ε_2 and ε_3, can be expressed in terms of maximum and minimum principal strains, ε_P, ε_Q, as follows in Eq. 8 [7]. In addition, in order to validate strain results, a Mohr's circle was also used [2].

$$\varepsilon_{P,Q} = \frac{\varepsilon_1+\varepsilon_2}{2} \pm \frac{1}{\sqrt{2}}\sqrt{(\varepsilon_1-\varepsilon_2)^2+(\varepsilon_2-\varepsilon_3)^2}$$

$$\theta = \frac{1}{2}\tan^{-1}\left(\frac{\varepsilon_1-2\varepsilon_2+\varepsilon_3}{\varepsilon_1-\varepsilon_3}\right) \quad (8)$$

Through the application of Eq. (8) to experimental data, some "stress-strain" graphs were drawn. In Fig. 6 it is possible to observe a typical graph that was obtained from the experimental tests, which is in accordance with a stress-strain curve given in the standard [6]. Additionally, in Table 1 is summarized the data gathered.

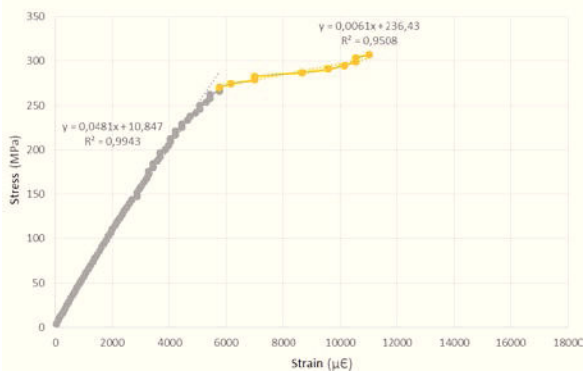

Fig. 6. Example of an experimental stress-strain curve drawn.

From the analysis of the stress-strain curves and the results presented in Table 1, it was possible to infer mean values for Young's modulus and for stress-strain values – both at transition and critical points, namely 48 GPa, (266 MPa, 5759 με) and (318 MPa, 17278 με), respectively.

Table 1. Summary of test results.

	E (GPa)	Transition point		Critical Point	
		σ (MPa)	ε (μЄ)	σ (MPa)	ε (μЄ)
Test 1	41.4	263	6000	308	14313
Test 2	38	265	6959	318	17278
Test 3	53.6	271	5429	322	17875
Test 4	50.2	270	5373	356	17834
Test 5	48.1	266	5759	307	11028
x̄±σ	48.1±6.1	266±3.4	5759±642	318±19	17278±2000

3.2. Internal pressure tests

Besides the experimental tests performed and described in the previous section, internal pressure tests were also carried out. Through a self-contained breathing apparatus, with an internal pressure equal to 20 MPa (source of pressure), a composite pressure vessel (Figs. 2 and 7) was pressurized. Two strain gauges rosettes (one applied in the main cylinder body and another in the dome of the pressure vessel) were used for the extensometry tests.

The pressure vessel was pressurised using increments of 200 Psi (1.38 MPa), until the maximum of 2400 Psi (16.5 MPa). At each stage, the strain values were measured through the 6 channels of the strain- gage rosettes.

Fig. 7. Internal pressure tests.

The results could be expressed by Fig. 8.

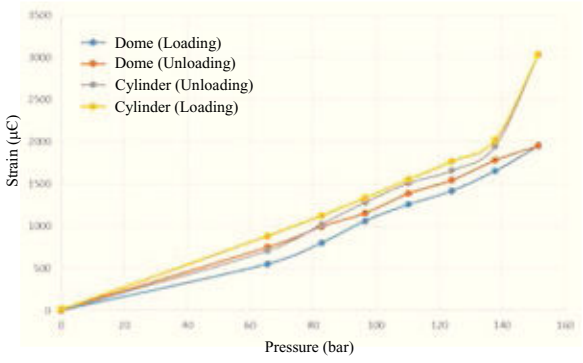

Fig. 8. Strain *versus* internal pressure.

3.3. Numerical simulations

Taking advantage of the experimental tests carried out, numerical simulations of composite specimens under axial tensile stress were considered (Fig. 9) in order to validate numerical simulations. The specimens were simulated both in *SolidWorks Simulation* and *ANSYS* software. The boundary conditions were: one edge, the shorter, supported, and the opposite edge loaded with a tensile load equal to 21 kN; in addition, one surface was considered as simply supported, in order to avoid bending. The specimen was modelled with 36 plies, each one with 0.13 mm thickness, and with a symmetric winding angle of 26.5º and -26.5º, as it was the real composite laminate. Comparing the results of the experimental tensile tests with those obtained in the numerical simulations, it was possible to conclude that strain values calculated were similar to the strain values measured, with a 4% maximum deviation.

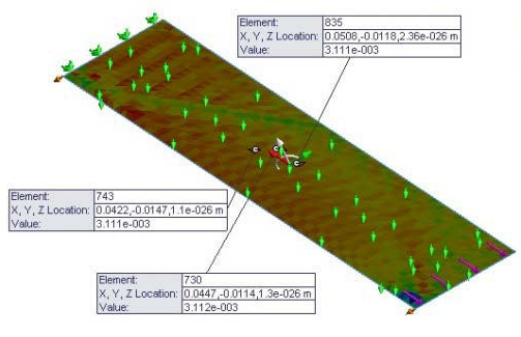

Fig. 9. FEA of a sample of CFRP: strain values (mm/mm).

4. Numerical Simulation of a SCBA Composite Pressure Vessel

A SCBA pressure vessel (Fig. 1) manufactured in a CFRP, with a constant thickness of 14 mm, calculated during the design phase (section 2.2, t_{HOOP}), was modelled and submitted to an internal pressure of 300 bar (30 MPa). Although the stresses calculated by FEA were lower than the critical allowable stress throughout the vessel (Table 1, 307 MPa), localized high tensile stresses were detected at the bottom of the SCBA where a stress field singularity was determined (Fig. 10 a)).

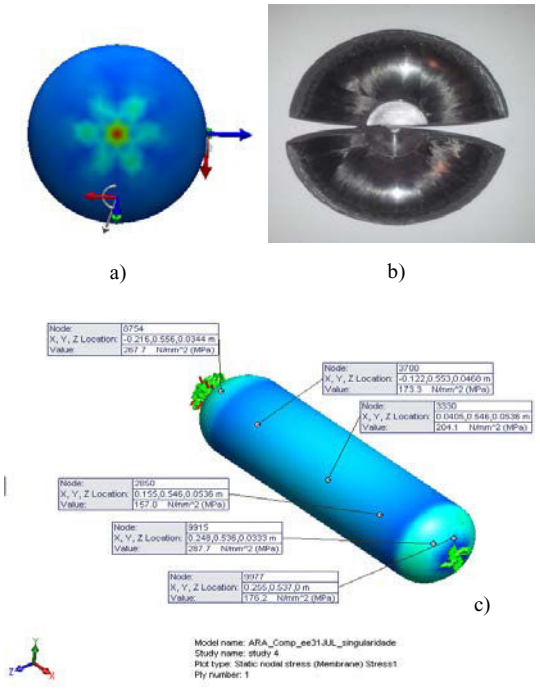

Fig. 10. a) FEA: stress field singularity calculated at the dome of SCBA; b) Region filled in with a metallic rod in order to remove stress field singularity; c) Equivalent stress distribution in the SCBA manufactured in CFRP.

The material at this region was then removed from the model and filled in with a small metallic rod (Fig. 10 b)) that could also be useful for the filament winding manufacturing process (either using geodesic or modified geodesic winding) [4]. Hence, the metallic rod's diameter should be equal or higher than 30 mm (Fig. 10 c)). Doing as described, stresses along SCBA main body slightly increased (not relevant), but the singularity disappeared (Fig. 10 c)).

5. Conclusions

Filament winding has been developed along the years and is considered the most efficient and appropriate process to manufacture SCBA made of composite materials. In addition, filament winding provides not only efficient ply deposition but also angle control, good ratio reinforcement/matrix, and allows mass production.

Particularly, in the study here presented, CFRP provided the possibility to produce safe and lightweight SCBA 6 times lighter than a metallic material SCBA made.

Some geometries of SCBA could contain a stress field singularity in its bottoms. Those singularities can be solved by applying some metallic reinforcements, like rivets in those zones, which in turn provide support for the winding process.

The stress values obtained by numerical simulation and experimental tests are similar to the design and analytic values, concluding thus that used design methodologies were coherent.

References

[1] A.C. Ugural (Ed.), Stresses in Plates and Shells, McGraw-Hill, New York, USA, 1981.
[2] ASME Boiler and Pressure Vessel Code – Section VIII, Division 1, 2013.
[3] L. Fernandes, Projeto de reservatórios sob pressão fabricados em materiais compósitos, Lisboa, Portugal, 2014.
[4] S. Peters (Ed.), Composite Filament Winding, ASM International, Ohio, USA, 2011.
[5] D. Gay, S.V. Hoa, S.W. Tsai (Ed.), Composite Materials – Design and Applications, CRC Press, London, UK, 2003.
[6] ASTM D3039/D 3039M, Standard test method for tensile properties of polymer matrix composite materials, ASTM International, USA, 2002.
[7] Tech Note TN-515, Strain Gage Rosettes: Selection, Application and Data Reduction, Micro Measurements – Vishay Precision Group, 2010.